Protective Role of Vitamin C in Wi-Fi Induced Oxidative Stress in MC3T3-E1 Cells in Vitro

Mengxi Wang [1,2], Guohui Yang [1], Yu Li [3], Qun Wu [1,*], and Yingsong Li [4]

[1] School of Electronic and Information Engineering, Harbin Institute of Technology, Harbin 150001, China

[2] The Fourth Affiliated Hospital of Harbin Medical University, Harbin 150001, China

[3] Department of Life Science and Engineering, Harbin Institute of Technology, Harbin 150001, China

[4] College of Information and Communication Engineering, Harbin Engineering University, Harbin 150001, China
*qwu@hit.edu.cn

Abstract ─ The increasing convenience and benefits provided by wireless technology innovations may also affect the human health because of Wi-Fi electromagnetic radiation. The effects of 2.45 GHz Wi-Fi on oxidative stress (OS) in MC3T3-E1 cells and the protective role of vitamin C are presented and analyzed in this paper. MC3T3-E1 cells were exposed to 100 mW and 500 mW 2.45 GHz Wi-Fi signals at specific absorption rates (SARs) of 0.1671 W/kg and 0.8356 W/kg, referred to as SARa and SARb, respectively, for 0-180 minutes to determine the optimal irradiation time by testing reactive oxygen species (ROS) and glutathione (GSH). Following irradiation for the optimal irradiation time, ROS levels were assayed for 0-120 min after each irradiation. Additional vitamin C is added to the medium to investigate the effect on ROS and GSH. A FDTD simulation showed that the cell layer temperature increased by 0.1°C and 0.5°C after being exposed in the SARa and SARb for the optimal irradiation time (90 min). Ninety min of Wi-Fi irradiation provoked an obvious increment in ROS and GSH on the first day, and the ROS level returned to the initial level 30 min after the irradiation; however, on the third day, it took 90-120 min for ROS to return to baseline. Vitamin C significantly reduced ROS levels and recovery times. In conclusion, 2.45 GHz Wi-Fi radiation triggered oxidative stress in osteoblasts 3cm from the source antenna. Vitamin C effectively reduced the ROS levels stimulated by nonthermal effects of Wi-Fi irradiation.

Index Terms ─ FDTD, in vitro, osteoblast, oxidative stress, temperature.

I. INTRODUCTION

Wi-Fi, a wireless network technique that emits radiation mostly at 2.45 GHz in the radio frequency (RF) range, affects the human body mainly through nonthermal effects [1]. However, several reports have addressed the problem of temperature measurements, since some researchers continue to believe that the biological effects of Wi-Fi irradiation can be attributed to increases in temperature [2]. The determination of whether the biological effects of Wi-Fi being caused by thermal or nonthermal effects requires a clear understanding of the temperature increase in biological tissue.

Bone is a metabolically active organ that continuously renews itself throughout life through a dynamic equilibrium dominated by three major types of bone cells: osteoclasts, osteoblasts and osteocytes [3]. Bone homeostasis can be disturbed by a variety of endogenous and exogenous factors, such as inflammation [4], loading [5], diabetes [6] and electromagnetic fields (EMFs) [7]. OS as a consequence of an oxidant-antioxidant imbalance favoring oxidants is the most direct response to a variety of adverse stimuli [8]. EMFs have been reported to increase the production or longer presence of free radicals which are the endogenous mechanism responsible for OS [9]. OS induced by Wi-Fi irradiation has been confirmed in the brain [10], liver [11], laryngotracheal mucosa [12] and uterus [13] in vivo experiments, and Çiğ B [14] found that the electromagnetic radiation (EMR) from Wi-Fi devices and mobile phones placed within 10 cm of cells induced OS in MCF-7 cells in vitro. In addition, vitamin C, an important free-radical scavenger, is considered to be an important inhibitor of Wi-Fi-related OS in the rat liver [11]. Thus, it is reasonable to presume that OS induced by Wi-Fi in osteoblasts might also be suppressed by vitamin C.

In this paper, the effects of 2.45 GHz Wi-Fi on OS in MC3T3-E1 cells and the protective role of vitamin C are presented and analyzed in detail. The contribution of this paper can be outlined as follows. (1) The specific

Submitted On: February 25, 2020
Accepted On: May 13, 2020

1054-4887 © ACES

absorption rates in the cell's were calculated in the 2.45 GHz Wi-Fi environment. (2) The temperature difference in the cell layer was analyzed. (3) Wi-Fi induced ROS and GSH changes were found. (4) The role of vitamin C in reducing OS was confirmed.

II. MATERIALS AND METHODS

A. Wi-Fi exposure settings

A laptop computer with Wi-Fi antenna, 60-mm cell culture dishes containing 4 mL of culture medium and a Wi-Fi router were placed in a Forma Series II 3110 Water Jacketed CO_2 Incubator (Thermo Fisher Scientific Inc., Waltham, USA) with 5% CO_2 at 37°C, as illustrated in Fig. 1. In the control group, the Wi-Fi router and computer were placed in the cell incubator in an open position without data transmission. The distance between culture dishes and router antennas is approximately 3 cm.

B. Thermal simulation

The FDTD method (Lumerica Solutions Inc., Vancouver, Canada) was employed to assess the SAR distribution in the cell monolayer. In the research of [15] the temperature of cells was carefully calculated with Debye's parameters of the cornea and aqueous humor by FDTD. However, it was confirmed by [16] that the effect of cell layers on the power delivery or heating of liquid is negligible. Consequently, the model in this research was simplified and the last layer (0.1 mm) of the culture medium was considered as the cell monolayer. The detailed steps and methods of FDTD was describe in [17] and [18]. The determination inside biological solution is expressed in terms of the specific absorption rate:

$$SAR = \frac{\sigma}{2\rho}\left|\vec{E}\right|^2. \quad (1)$$

Where E is the root-mean-square local electric field strength (V/m), σ is the electric conductivity (S/m), and ρ is the sample density (kg/m3). If the electric field components of a point (i, j, k) in an organism are Ex, Ey and Ez respectively, the distributional SAR can be calculated by the following formula (2), expressed in $SAR(\vec{r})$, which is defined as the electromagnetic power absorbed per unit mass of a biological tissue at a distance $\vec{r}$ adjacent to at any point:

$$SAR(\vec{r}) = \frac{1}{2\rho(i,j,k)}\left[\sigma_x(i,j,k)E_x^2(i,j,k) + \sigma_y(i,j,k)E_y^2(i,j,k) + \sigma_z(i,j,k)E_z^2(i,j,k)\right]. \quad (2)$$

The dielectric and material thermal parameters at 37°C and 2.45 GHz are given in Table 1. The temperature of the surrounding atmosphere was assumed to be stable at 37°C. The voxel size was 0.1 mm, and the time step was 0.1 seconds. The last layer (height 0.1 mm) of the culture medium was considered the cell monolayer. The specific absorption rates are 0.1671 W/kg and 0.8356 W/kg for 100 mW and 500 mW Wi-Fi radiation, referred to as SARa and SARb, respectively.

The thermodynamics equation was used to determine the temperature increase in the cell monolayer at the bottom of the culture dishes. The thermodynamics equation is as follows [20]:

$$C\rho\frac{dT}{dt} = K\nabla^2 T + \rho(SAR) - BT. \quad (3)$$

Where T is the temperature (K), C is the specific heat capacity ($J.K^{-1}.kg^{-1}$), K is the thermal conductivity ($W.m^{-1}.K^{-1}$), B is a parameters related to blood flow.

The boundary condition is:

$$H \cdot (T_s - T_c) = -K\frac{\partial T}{\partial n}. \quad (4)$$

Where H is Convection coefficient, T_s is surface temperature, and Tc is air temperature.

For the spatial continuity function F(x,y,z,t), the discrete form of its time step at m can be written as follows:

$$F^m(i,j,k) = F(i\delta x, j\delta y, k\delta z, m\delta t). \quad (5)$$

Where δ is the space step, δt is the time step.

(3) and (4) come to:

$$T^{m+1}(i,j,k) = T^m(i,j,k) + \frac{\delta_t}{C\rho(i,j,k)}SAR(i,j,k) - \frac{\delta_t * b(i,j,k)}{\rho(i,j,k)C\rho(i,j,k)} * [T^m(i,j,k) - Tb] + \frac{\delta_t * K(i,j,k)}{\rho(i,j,k)C\rho(i,j,k)\delta^2} * [T^m(i+1,j,k) + T^m(i,j+1,k) + T^m(i,j,k+1) + T^m(i-1,j,k) + T^m(i,j-1,k) + T^m(i,j,k-1) - 6T^m(i,j,k)], \quad (6)$$

$$T^{m+1}(i_{min},j,k) = \frac{KT(i_{min}+1,j,k)}{K+h\delta} + \frac{T_a h\delta}{K+h\delta}, \quad (7)$$

δt satisfies the condition:

$$\delta t \le \frac{2\rho C\rho\delta^2}{12K+b\delta^2}. \quad (8)$$

Figure 2 (a) shows a temperature comparison for Wi-Fi EMF radiation powers of 100 mW and 500 mW after 90 min of irradiation in the cell layer. The mean temperature increases under the 100 mW mode and 500 mW mode were approximately 0.1°C and 0.5°C respectively at 90 min (Fig. 2).

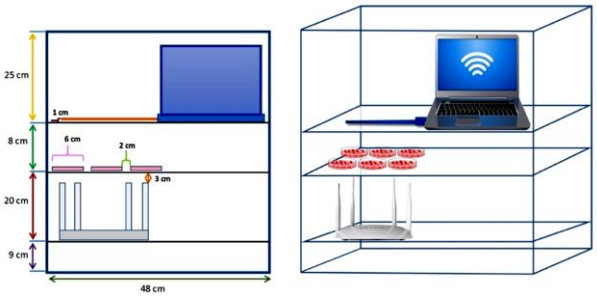


Fig. 1. Layout of cell dishes, the Wi-Fi router and the laptop computer in the cell incubator.

C. Cell culture

MC3T3-E1 cells (iCell Bioscience Inc., Shanghai, China) of the clone-14 preosteoblastic murine cell line were cultured in α-MEM containing 10% newborn bovine

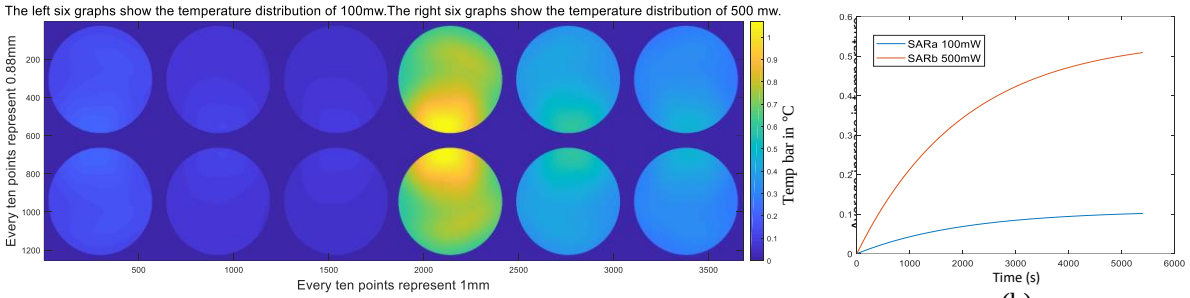
serum, 100 IU/mL penicillin and 100 µg/mL streptomycin under saturating humidity, 5% CO_2 and 37°C. The medium was changed every 48 h. When the cells reached approximately 80% confluence, they were digested with 0.25% trypsin (Gibco Inc., Grand Island, USA), diluted and then subcultured at a 1:3 ratio.

D. In vitro differentiation

For this step, 10 mmol/L β-phospho-glycerol, 10^{-8} mol/L dexamethasone and 50 µg/mL ascorbic acid (vitamin C) were added to the above culture medium to make osteogenic medium which was changed every 48 h.

E. Experimental groups

To select the optimum daily irradiation time, the cells were exposed to radiation after 72 h of induced differentiation, and each group contained at least three samples. The cells were divided into six groups: (i) 0 min, (ii) 30 min, (iii) 60 min, (iv) 90 min, (v) 120 min, and (vi) 180 min. These groups were further subdivided into sham, SARa 2.45 GHz Wi-Fi, and SARb 2.45 GHz Wi-Fi groups.



(a) (b)

Fig. 2. The simulation result of temperature in the cell layer: (a) temperature difference after 90 min of irradiation in the cell layer, and (b) temperature dynamics within a cell monolayer.

Table 1: Electrical properties and thermal paramters of materials at 37°C 2.45 GHz [15-16], [19]

	ε_r	σ (Sm^{-1})	C ($kJ(kg°C)^{-1}$)	K ($W(km)^{-1}$)	ρ (kgm^{-3})
Medium	71	2.5	4.2	0.6	1000
Petri dish	2.5	0.001	0.12	L2	1100

To measure GSH/ROS after radiation, the cells were exposed to Wi-Fi radiation for the optimum irradiation time each day for 1 to 3 days in 3 groups: (i) sham, (ii) SARa 2.45 GHz Wi-Fi, and (iii) SARb 2.45 GHz Wi-Fi. Tests were performed at 0 min, 15 min, 30 min, 45 min, 60 min, 90 min, and 120 min after Wi-Fi irradiation.

F. ROS

After 72 h of induction in osteogenic medium, the cells were digested with 0.25% trypsin-0.53 mM EDTA and then seeded into a 96-well plate at a density of 5×103 cells/mL in 100 µL of osteogenic medium, which was changed every 48 h. 2',7'-Dichlorofluorescein diacetate (KeyGen Biotech Co., NanJing, China) was added to each well according to the instructions. After 45 min of incubation in the dark, the cells were exposed to Wi-Fi radiation. ROS levels were determined by measuring the fluorescence intensity at 518-nm excitation and 605-nm emission using a spectrophotometer plate reader (Spectra Max M3, Molecular Devices, California, USA).

G. GSH

Cells were seeded in 60-mm culture dishes at a density of 5×104 cells/mL in 4 mL of osteogenic medium, which was changed every 48 h. Seventy-two hours later, the cells were exposed to Wi-Fi radiation. Then, the cells were digested with 0.25% trypsin-0.53 mM EDTA. After centrifugation (3500 g, 10 min), the cell supernatant was added to a 96-well culture plate. Cellular GSH was determined using a GSH assay kit (KeyGen Biotech Co.) according to the manufacturer's instructions. The optical absorbance values were measured with a microplate reader at 405 nm (SpectraMax M3).

H. Statistical analysis

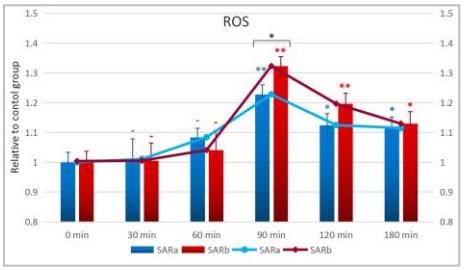
The data are expressed as the mean ± standard deviation (SD) of three or more independent experiments. Significant differences were determined through factorial analysis of variance (ANOVA). Statistical analysis was performed using SPSS 13.0 software (SPSS Inc., Chicago, USA). A P-value<0.05 was considered statistically significant.

III. RESULTS

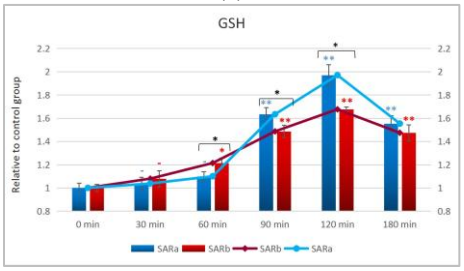
A. Determining the optimum irradiation time for further experiments (Fig. 3)

The cells were exposed to Wi-Fi radiation for 0-180 min after being induced for 72 h in osteogenic medium,

and ROS and GSH levels were measured immediately after irradiation. ROS levels in both the SARa group and SARb group were largely unaltered in the first 60 min. Although an upward trend was observed from 30 to 60 min, the changes at the 30th and 60th minutes were not significantly different in either the SARa or SARb group compared with the control group. From the 60th minute onward, the ROS level increased rapidly, peaked at the 90th minute, and then began to decrease but remained higher than in the control group at the 180th minute. ROS levels in the SARb group were significantly higher than in the SARa group at the 90th min but not at the other times. The peak GSH level was recorded at the 120th min. Significant differences between the SARa and SARb groups were detected at the 60th, 90th and 120th minutes, and the GSH levels of the SARa group were higher than those of the SARb group, except at the 60th minute. Unlike the GSH level in the SARb group, the GSH level in the SARa group increased significantly as early as the 60th minute. At the 180th minute, the GSH and ROS levels were still much higher than the original levels. We chose 90 min as the daily optimum irradiation time for the subsequent experiments since the ROS levels in both the SARa and SARb groups were highest at the 90th minute. In addition, both ROS and GSH levels differed significantly between the SARa and SARb groups, between the SARa and control groups, and between the SARb and control groups at the 90th minute.



(a)

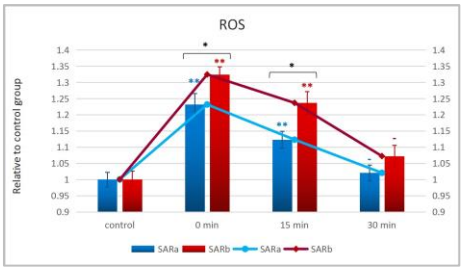


(b)

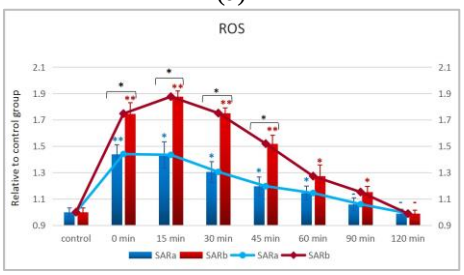
Fig. 3. ROS and GSH levels during Wi-Fi exposure: (a) relative ROS levels at 0/30/60/90/120/180 min of Wi-Fi exposure, and (b) relative GSH levels at 0/30/60/90/120/180 min of Wi-Fi exposure (P≥0.05 -, P<0.05 *, P<0.01 **).

B. Changes in ROS 0-30 min after Wi-Fi irradiation for the optimum irradiation time (Fig. 4 (a))

MC3T3-E1 cells were exposed to Wi-Fi radiation for 90 min after 72 h of differentiation. ROS were measured 0-30 min after irradiation was completed. The measurement taken immediately after irradiation was defined as 0 min. ROS levels began to decrease at the time at which irradiation stopped and took 30 min to return to the original level. ROS levels in the SARb group were significantly higher than those in the SARa group at 0 and 15 min. Even though the ROS level at 30 min after irradiation did not completely recover in either the SARa or SARb group, this difference can be ignored because these levels were not significantly different from the control level.



(a)



(b)

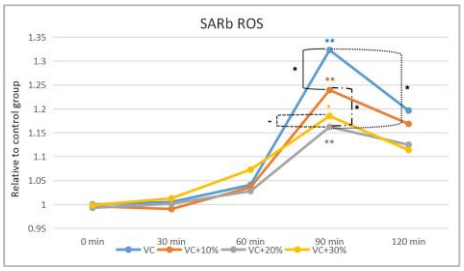
Fig. 4. ROS levels after Wi-Fi exposure: (a) relative ROS levels after Wi-Fi exposure for 90 min, and (b) relative ROS levels after Wi-Fi exposure for 90 min/day for 3 days (P≥0.05 -, P<0.05 *, P<0.01 **).

C. Changes in ROS after Wi-Fi irradiation for the optimum irradiation time every day for 3 days (Fig. 4 (b))

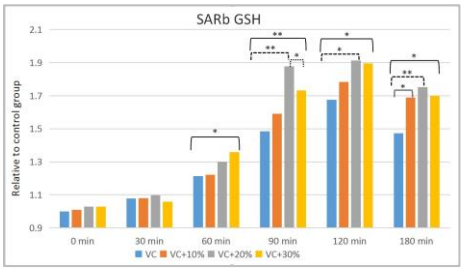
After 72 h of differentiation, MC3T3-E1 cells were exposed to 90 min of Wi-Fi radiation for 3 days. ROS were measured after the 3rd day of irradiation. The time point immediately after irradiation was defined as 0 min. ROS levels increased slightly after irradiation was stopped and took 120 min or 90 min to decrease to control levels in the SARb and SARa groups, respectively. The ROS levels of the SARb group were significantly higher than those of the SARa group at 0 min, 15 min, 30 min and 45 min after Wi-Fi irradiation.

D. Determining the optimum concentration of vitamin C by repeating experiment 1 in the SARb group with extra vitamin C in the induction culture medium (Fig. 5)

The results of experiments A, B and C show that the peak ROS level was higher in the SARb group than in the SARa group and that recovery was slower in the SARb group than in the SARa group. Thus, our subsequent studies were performed under the SARb conditions. We adjusted the concentration of vitamin C in the induction medium from 50 μg/mL to 55 μg/mL, 60 μg/mL or 65 μg/mL and then repeated experiment 1 to examine ROS and GSH in the SARb group. After 60 min of irradiation, ROS levels increased in all vitamin C groups, peaked at the 90th minute, and then decreased to basal levels. The ROS level at the 90th minute was inversely proportional to the vitamin C concentration (50 μg/mL to 60 μg/mL) and was significantly different from the level in the control group. However, the ROS level in the presence of 65 μg/mL vitamin C was lower than in the presence of 60 μg/mL vitamin C at the 90th minute, but the difference was not significant. At the 90th minute, GSH levels in the 60 μg/mL group were also higher than those in the other groups. Therefore, we adopted 60 μg/mL as the optimum concentration of vitamin C.



(a)



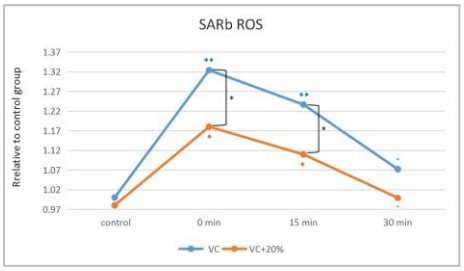
(b)

Fig. 5. ROS and GSH levels in the SARb group during Wi-Fi irradiation with extra vitamin C in the induction medium: (a) relative ROS levels in the SARb group at 0/30/60/90/120 min of Wi-Fi exposure with 10-30% extra vitamin C in the induction medium, and (b) relative GSH levels in the SARb group at 0/30/60/90/120/180 min of Wi-Fi exposure with 10-30% extra vitamin C in the induction medium (P≥0.05 -, P<0.05 *, P<0.01 **).

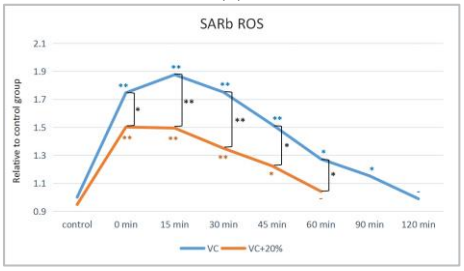
E. Changes in ROS in the SARb group 0-30 min after Wi-Fi irradiation for the optimum irradiation time with the optimum concentration of vitamin C in the induction medium (Fig. 6 (a))

Experiment B was repeated with 60 μg/mL vitamin C in the induction medium to measure the ROS in the SARb group. The measurement performed immediately after 90 min of Wi-Fi exposure was considered 0 min. The ROS levels in the vitamin C and vitamin C+20% control groups were not significantly different, but the ROS levels in the 50 μg/mL vitamin C experimental group were significantly higher than those in the 60 μg/mL vitamin C experimental group at both 0 and 15 min.

F. Changes in ROS in the SARb group 0-120 min after Wi-Fi irradiation for the optimum irradiation time for 3 days with the optimum concentration of vitamin C in the induction medium (Fig. 6 b))



(a)



(b)

Fig. 6. ROS levels in the SARb group after Wi-Fi exposure with 20% extra vitamin C in the induction medium: (a) relative ROS levels in the SARb group after 90 min/day of Wi-Fi exposure with 20% extra vitamin C in the induction medium, and (b) relative ROS levels in the SARb group after 90 min/day of Wi-Fi exposure for 3 days with 20% extra vitamin C in the induction medium. (P≥0.05 -, P<0.05 *, P<0.01 **).

Experiment C was repeated with 60 μg/mL vitamin C in the induction medium to measure ROS in the SARb groups. The time point immediately after 90 min of Wi-Fi exposure was considered 0 min. ROS levels in the vitamin C+20% experimental groups at 0 min, 15 min, 30 min and 45 min were higher than those in the vitamin

C+20% control group, while the ROS levels in the vitamin C experimental groups at 0 min, 15 min, 30 min, 45 min, 60 min and 90 min were higher than those in the vitamin C control group. The ROS levels of the 50 μg/mL vitamin C group at 0 min, 15 min, 30 min, 45 min and 60 min were significantly higher than those of the 60 μg/mL vitamin C group. Therefore, the ROS recovery time in the 60 μg/mL vitamin C groups was half that in the 50 μg/mL vitamin C groups.

IV. DISCUSSIONS

The safety standard of non ionizing radiation was set mainly focusing on whether it exerts obvious thermal effects on the human body over a certain period of time [21], but without considering nonthermal or cumulative effects. Thus, even within the recommended values, adverse effects of Wi-Fi radiation on certain types of cells or organs have been verified [13]. Non ionizing EMR can alter the energy level and spin orientation of electrons and, consequently, increase the activity, concentration and lifetime of ROS [14]. OS stimulated by Wi-Fi irradiation for a period from 5 days [11] to 6 months [22] has been found in some important organs deep in rats' body. In the vitro experiment, [14] set 6 tubes of MCF-7 breast cancer cells at different distances (0 cm, 1 cm, 5 cm, 10 cm, 20 cm and 25 cm) from a radiant for 1 h. The mean SAR of the 6 tubes was 0.36±0.02 W/kg under 900 MHz exposure at 12 μW/cm2. Çiğ B found that cytosolic ROS production, Ca^{2+} concentrations, apoptosis, and caspase-3 and caspase-9 levels were higher in all the mobile phone and 2.45 GHz Wi-Fi groups at distances of less than 10 cm. An increase in ROS in a osteoblasts monolayer exposed to Wi-Fi radiation (3 cm from router antennas) was also found in our work, and Wi-Fi radiation was clearly shown to be an exogenous OS stimulus. Our main concern is the duration of ROS generation and the return of ROS to baseline levels. ROS did not increase until 90 min after the initial exposure to Wi-Fi, which may be attributed to "window effects" [23]. Even with continuing irradiation, ROS did not increase and instead decreased from 90 to 180 min because of the increase in GSH which, as an antioxidant, serves as a natural defense mechanism to restore the dynamic balance between ROS generation and elimination in cells [24].

ROS levels in the SARb group were higher than those in the SARa group in experiments 1, 2 and 3 and showed an SAR-dependent pattern similar to that found in other studies [25]. The ROS level returned to baseline within 30 min of the initial exposure to Wi-Fi; however, after the third day of radiation, this return took 90 min in the SARa group and 120 min in the SARb group, which could be interpreted as a "cumulative effect" [26]. Prolonged exposure times and increased exposure doses may reasonably be concluded to make it increasingly difficult to restore ROS levels to normal. The mechanism by which EMFs increase ROS is partly attributing to the decreased efficiency of antioxidant mechanisms [27]. However, in our study, GSH rapidly increased even before ROS levels changed, which might play an important part in ROS regulation during Wi-Fi exposure. Similarly, in a study by [28], V79 fibroblast cells were exposed 1800 MHz RF (SAR 1.6 W/kg) generated in a gigahertz transverse electromagnetic mode (GTEM) cell, and GSH levels were found to increase immediately after 10 min of exposure, but ROS increased only after 60 min of exposure. Cermak AMM suggested that short-term RF exposure resulted in a transient oxidation-reduction imbalance in fibroblast cells following adaptation to the applied experimental conditions. [29] also found that ROS increased in osteoblasts after a single exposure to extremely low-frequency pulsed electromagnetic fields (ELF-PEMFs) and that GSH did not decrease; these changes essentially represented an antioxidant defense mechanism in which ELF-PEMF stimulated the cells to produce a small amount of harmless ROS to improve osteoblast function and activity. Hence, the ROS and GSH increases observed in our study may similarly be a protective mechanism elicited by Wi-Fi irradiation.

If Wi-Fi exposure is inevitable, then it is particularly important to explore ways to reduce ROS and minimize the risk of side effects. Various antioxidant mechanisms have been confirmed to neutralize the harmful effects of ROS in cells, among which vitamin C, a free-radical scavenger in extracellular fluids, is considered to be an important inhibitor of Wi-Fi-related OS in rats [11]. The original culture medium for osteoblasts contains vitamin C, which may be another factor that reduces ROS and/or accelerates the reduction of ROS levels. High levels of GSH might be related to the fact that vitamin C can reduce oxidized GSH (GSSG) into GSH. Accordingly, we added different concentrations of extra vitamin C to the culture medium and found that 60 μg/mL was the most appropriate concentration for limiting ROS and upregulating GSH. This optimum concentration of vitamin C significantly reduced ROS levels and shortened the recovery time by half (from 120 to 60 min) after the 3rd day of Wi-Fi irradiation. Furthermore, the ROS levels of the different vitamin C groups were inversely proportional to the GSH level of the same groups, further supporting a mechanism whereby GSH plays an important role in ROS regulation during Wi-Fi exposure and is upregulated by vitamin C.

V. CONCLUSIONS

The long-term and close-range Wi-Fi EMF radiation slightly increases the temperature in a cell monolayer, however the temperature variation (no more than 1°C) is too small to induce the cell biological reaction. Hence, it is believed that the effect of Wi-Fi irradiation on cells would be stimulated by nonthermal effects.

The SARs of Wi-Fi EMF is far below the safety

standard of non ionizing radiation, but still elevates ROS in cells after long-term exposure. Therefore, Wi-Fi EMF could be an exogenous OS stimulus and affect bone homeostasis. Furthermore, the longer the irradiation time and the stronger the radiation, the more obvious the effect on osteoblasts. However, short-term exposure (less than 60 min) can neither change the level of ROS nor GSH owing to "window effects".

ROS induced by Wi-Fi EMF radiation can be eliminated by endogenous or Wi-Fi induced GSH, which acts as a protective mechanism of osteoblasts. Nevertheless, it takes longer times for osteoblasts to eliminated ROS with the increase of exposure doses due to the "cumulative effect".

Vitamin C effectively reduces ROS levels and recovery times by increasing GSH, and its effect shows a concentration-dependent pattern at low concentrations.

Due to the limited experimental conditions, the radiation distance setting is an extreme case (a cell layer 3cm from the source antenna), and the influence of distance change on the result needs further study. In the future, we will consider the MIMO antenna and circular polarization antenna [30-34] and arrays [35] in the experiment and use the adaptive filtering [36-41] to suppress the noises and improve the performance.

ACKNOWLEDGMENTS

This study was funded by the National Natural Science Foundation of China (61571155); the Natural Science Foundation of Heilongjiang Province, China (QC2015124), and the Fundamental Research Funds for the Central Universities (3072020CFT0802).

REFERENCES

[1] M. B. Salah, H. Abdelmelek, and M. Abderraba, "Wifi and health: Perspectives and risks," no. 1, pp. 012-022, 2017.

[2] S. S. Lee, H. R. Kim, M. S. Kim, et al., "Influence of smartphone Wi-Fi signals on adipose-derived stem cells," *J. Craniofac Surg*., vol. 25, no. 5, pp. 1902-1907, 2014.

[3] V. Domazetovic, G. Marcucci, T. Iantomasi, et al., "Oxidative stress in bone remodeling: Role of antioxidants," *Clin. Cases Miner. Bone Metab*., vol. 14, no. 2, pp. 209-216, 2017.

[4] W. Razawy, M. van Driel, and E. Lubberts, "The role of IL-23 receptor signaling in inflammation-mediated erosive autoimmune arthritis and bone remodeling," *Eur. J. Immunol*., vol. 48, no. 2, pp. 220-229, 2018.

[5] S. A. Murshid, "The role of osteocytes during experimental orthodontic tooth movement: A review," *Arch. Oral Biol*., vol. 73, pp. 25-33, 2017.

[6] A. G. D. Vianna, C. P. Sanches, and F. C. Barreto, "Effects of type 2 diabetes therapies on bone metabolism," *Diabetol. Metab. Syndr*., vol. 9, no. 1, 2017.

[7] M. Zhai, D. Jing, S. Tong, et al., "Pulsed electromagnetic fields promote in vitro osteo-blastogenesis through a Wnt/β-catenin signaling-associated mechanism," *Bioelectromagnetics*, vol. 37, no. 3, pp. 152-162, 2016.

[8] V. Selvaraju, M. Joshi, S. Suresh, et al., "Diabetes, oxidative stress, molecular mechanism, and cardio-vascular disease–An overview," *Toxicol. Mech. Methods*, vol. 22, no. 5, pp. 330-335, 2012.

[9] M. Simko, "EMF and the redox homeostasis: The link to cell activation processes," *Toxicology Letters*, ID:280 S32, 2017.

[10] H. Othman, M. Ammari, K. Rtibi, et al., "Postnatal development and behavior effects of in-utero exposure of rats to radiofrequency waves emitted from conventional WiFi devices," *Environ. Toxicol. Pharmacol*., vol. 52, pp. 239-247, 2017.

[11] F. Shekoohi-Shooli, S. M. J. Mortazavi, M. B. Shojaei-Fard, et al., "Evaluation of the protective role of vitamin c on the metabolic and enzymatic activities of the liver in the male rats after exposure to 2.45 GHz of Wi-Fi routers," *J. Biomed. Phys. Eng*., vol. 6, no. 3, ID:157, 2016.

[12] G. Aynali, M. Nazıroğlu, Ö. Çelik, et al., "Modulation of wireless (2.45 GHz)-induced oxidative toxicity in laryngotracheal mucosa of rat by melatonin," *Eur. ArcH. Oto-rhino-L*, vol. 270, no. 5, pp. 1695-1700, 2013.

[13] M. Yüksel, M. Nazıroğlu, M. O. Özkaya, "Long-term exposure to electromagnetic radiation from mobile phones and Wi-Fi devices decreases plasma prolactin, progesterone, and estrogen levels but increases uterine oxidative stress in pregnant rats and their offspring," *Endocrine*, vol. 52, no. 2, pp. 352-362, 2015.

[14] B. Çiğ and M. Nazıroğlu, "Investigation of the effects of distance from sources on apoptosis, oxidative stress and cytosolic calcium accumulation via TRPV1 channels induced by mobile phones and Wi-Fi in breast cancer cells," *BBA-Biomem-branes*, vol. 1848, no. 10, pp. 2756-2765, 2015.

[15] J. Zhao, "In vitro dosimetry and temperature evaluations of a typical millimeter-wave aperture-field exposure setup," *IEEE Transactions on Microwave Theory and Techniques*, vol. 60, no. 11, pp. 3608-3622, 2012.

[16] M. Zhadobov, S. I. Alekseev, R. Sauleau, et al., "Microscale temperature and SAR measurements in cell monolayer models exposed to millimeter waves," *Bioelectromagnetics*, vol. 38, no. 1, pp. 11-21, 2016.

[17] A. Collin, M. Cueille, A. Perrin, et al., "Electro-magnetic dosimetry and thermal analysis of a new exposure setup for in vitro studies on a large frequency band," *Microwave Symposium, IEEE/ MTT-S International*, pp. 2221-2224, 2017.

[18] A. Paffi, M. Liberti, F. Apollonio, et al., "In vitro exposure: Linear and non-linear thermodynamic events in Petri dishe," *Bioelectromagnetics*, vol. 36, no. 7, pp. 527-537, 2015.

[19] M. Zhadobov, R. Augustine, R. Sauleau, et al., "Complex permittivity of representative biological solutions in the 2–67 GHz range," *Bioelectromagnetics*, vol. 33, no. 4, pp. 346-355, 2016.

[20] A. Hirata and T. Shiozawa, "Correlation of maximum temperature increase and peak SAR in the human head due to handset antennas," *IEEE Transactions on Microwave Theory and Techniques*, vol. 51, no. 7, pp. 1834-1841, 2003.

[21] ICNIRP, International Commission of Non-Ionizing Radiation Protection. Guidelines for limiting exposure to time-varying electric, magnetic and electromagnetic fields, URL: http://www.icnirp.de/documents/emfgdl.pdf

[22] A. Özorak, M. Nazıroğlu, Ö. Çelik, et al., "Wi-Fi (2.45 GHz)-and mobile phone (900 and 1800 MHz)-induced risks on oxidative stress and elements in kidney and testis of rats during pregnancy and the development of offspring," *Biol. Trace Elem. Res.*, vol. 156, no. 1-3, pp. 221-229, 2013.

[23] J. Zhou, L. G. Ming, B. F. Ge, et al., "Effects of 50 Hz sinusoidal electromagnetic fields of different intensities on proliferation, differentiation and mineralization potentials of rat osteoblasts," *Bone*, vol. 49, no. 4, pp. 753-761, 2014.

[24] H. Wang and X. Zhang, "Magnetic fields and reactive oxygen species," *Int. J. Mol. Sci*., vol. 18, no. 10, 2017.

[25] G. N. De Iuliis, R. J. Newey, B. V. King, et al., "Mobile phone radiation induces reactive oxygen species production and DNA damage in human spermatozoa in vitro," *PLOS ONE*, vol. 4, no. 7, 2009.

[26] H. S. Kim, J. S. Park, Y. B. Jin, et al., "Effects of exposure to electromagnetic field from 915 MHz radiofrequency identification system on circulating blood cells in the healthy adult rat," *Bioelectromagnetics*, vol. 39, no. 1, pp. 68-76, 2018.

[27] J. Espino, I. Bejarano, S. D. Paredes, et al., "Protective effect of melatonin against human leukocyte apoptosis induced by intracellular calcium overload: Relation with its antioxidant actions," *J. Pineal. Res*., vol. 51, no. 2, pp. 195-206, 2011.

[28] A. M. M. Cermak, I. Pavicic, B. T. Lovakovic, et al., "In vitro non-thermal oxidative stress response after 1800 MHz radiofrequency radiation," *GEN Physiol. Biophys*., vol. 36, no. 4, pp. 407-414, 2017.

[29] S. Ehnert, A. K. Fentz, A. Schreiner, et al., "Extremely low frequency pulsed electromagnetic fields cause antioxidative defense mechanisms in human osteoblasts via induction of O_2^- and H_2O_2," *Sci. Rep*., vol. 7, no. 1, ID: 14544, 2017.

[30] K. Yu, Y. Li, and X. Liu, "Mutual coupling reduction of a MIMO antenna array using 3-D novel meta-material structures," *Appl. Comput. Electromagn. Soc. J*., vol. 33, no. 7, pp. 758-763, 2018.

[31] J. Jiang, Y. Xia, and Y. Li, "High isolated X-band MIMO array using novel wheel-like metamaterial decoupling structure," *Appl. Comput. Electromagn. Soc. J*., vol. 34, no. 12, pp. 1829-1836, 2019.

[32] S. Luo, Y. Li, Y. Xia, and L. Zhang, "A low mutual coupling antenna array with gain enhancement using metamaterial loading and neutralization line structure," *Applied Computational Electromagnetics Society Journal*, vol. 34, no. 3, pp. 411-418, 2019.

[33] S. Luo, Y. Li, Y. Xia, et al., "Mutual coupling reduction of a dual-band antenna array using dual-frequency metamaterial structure," *Applied Computational Electromagnetics Society Journal*, vol. 34, no. 3, pp. 403-410, 2019.

[34] K. L. Chuang, X. Yan, Y. Li, and Y. Li, "A Jia-shaped artistic patch antenna for dual-band circular polarization," *AEÜ- International Journal of Electronics and Communications*, vol. 120,10.1016/j.aeue.2020.153207.

[35] X. Zhang, T. Jiang, and Y. Li, "A novel block sparse reconstruction method for DOA estimation with unknown mutual coupling," *IEEE Communications Letters*, vol. 23, no. 10, pp. 1845-1848, 2019.

[36] T. Jiang, T. Jiao, and Y. Li, "A low mutual coupling MIMO antenna using periodic multi-layered electromagnetic band gap structures," *Applied Computational Electromagnetics Society Journal*, vol. 33, no. 3, 2018.

[37] Y. Li, Z. Jiang, O. M. Omer-Osman, et al., "Mixed norm constrained sparse APA algorithm for satellite and network echo channel estimation," *IEEE Access*, vol. 6, pp. 65901-65908, 2018.

[38] Y. Li, Y. Wang, and T. Jiang, "Sparse-aware set-membership NLMS algorithms and their application for sparse channel estimation and echo cancelation," *AEU - International Journal of Electronics and Communications*, vol. 70, no. 7, pp. 895-902, 2016.

[39] Q. Wu, Y. Li, Y. V. Zakharov, et al., "A kernel affine projection-like algorithm in reproducing kernel hilbert space," *IEEE Transactions on Circuits and Systems II: Express Briefs*, 10.1109/TCSII.2019.2947317.

[40] B. Chen, Z. Li, Y. Li, and P. Ren, "Asymmetric correntropy for robust adaptive filtering," *IEEE Signal Processing Letters*, arXiv preprint arXiv: 1911.11855.

[41] W. Shi, Y. Li, and B. Chen, "A Separable maximum correntropy adaptive algorithm," *IEEE Transactions on Circuits and Systems II: Express Briefs*, 10.1109/TCSII.2020.2977608.